Theoretical description of deuteron-nucleus reactions using Optical Model

Author: Alex Teruel Piñol
Facultat de Física, Universitat de Barcelona, Diagonal 645, 08028 Barcelona, Spain.

Advisor: Xavier Viñas Gausí

Abstract: Total reaction cross section and elastic scattering angular distributions in deuteron-nucleus reactions is studied for nuclei in the mass range A = 9-209 and deuteron with incident energies from 12 up to 200 MeV, using a global parametrization optical model potential. The theoretical results are compared with the experimental data to verify the goodness of the model.

I. INTRODUCTION

The nucleon-nucleon (NN) interaction is the essential ingredient to describe the structure and dynamics of the atomic nucleus. The bare NN interaction can be determined quite precisely from the nucleon-nucleon scattering data and from the deuteron properties. Its use in more complicated scenarios where many nucleons are involved, such as nuclear reactions, becomes a highly complex mathematical problem. Thus, it is interesting to devise a model that allows to obtain reasonable results through simplified calculations. In this context, the optical model (OM), which is based in the assumption that the nucleon-nucleus interaction can be substituted by a complex mean-field potential (OMP), is a very useful tool to study nuclear reactions [1]. The real part of the OMP is in charge of describing the shape elastic scattering while the imaginary part is related with the various inelastic process that may occur and remove particles from the elastic channel.

The OMP can be determined from a theoretical basis or using a phenomenological approach. In this latter case, one starts choosing a determined analytical form, usually of Woods-Saxon type, which depend on 15-25 free parameters. These parameters are determined through a chi-square (χ^2) minimization procedure to reproduce, as well as possible, a given set of experimental data of differential and total cross-sections and analyzing powers. Besides, the OMP can be global or local. In the global case the OMP parameters become functions of the atomic number and mass number of the target nucleus, as well as of the projectile incident energy. Conversely, when the fit of the parameters is realized for a particular nucleus and energy, we have a local parametrization OMP. However, in this paper we will concentrate on the global potentials.

The successful results obtained by several local and global parametrizations OMP to describe nucleon-nucleus interactions (e.g. Varner *et al.* [2], Becchetti-Greenlees [3] and Koning-Delaroche [4]) have led other authors to consider an OMP for the interaction of composite particles with nuclei. In particular, we are interested in deuteron-nucleus reactions. One of the reasons why studying deuteron interactions is its usefulness in non-conventional radionuclides production, which is interesting to study because of its application to nuclear medicine. We can see an example of this in Ref. [5], where researchers try to determine the advantages (or disadvantages) of using deuterons to produce radionuclides instead of using protons or neutrons. Another reason is the possible utility of deuteron in nuclear fusion reactions, e.g. the fusion of a deuteron and a triton producing He-4 with a large release of energy, which could be used in nuclear fusion reactors.

Currently available global parametrizations OMP for the deuteron-nucleus elastic scattering have been obtained by Daehnick *et al.* (1980) [6], Bojowald *et al.* (1988) [7] and Han *et al.* (2006) [8]. In this work we will be focused on the study of total reaction cross sections and elastic scattering angular distributions in deuteron-nucleus reactions using Han *et al.* global parametrization OMP. The theoretical model will be used to analyze experimental data not included in the fit of this OMP with the aim to verify its prediction ability. Experimental data will be taken from EXFOR database [9].

II. THE OPTICAL MODEL POTENTIAL

The global parametrization of the OMP used in this work was enunciated by Han, Shi and Shen [8]. They obtained the parameters of the model by fitting the experimental data of total reaction cross section and elastic scattering angular distributions in the mass range of A=12-209 with incident deuteron energies up to 200 MeV.

The OMP analytical expression is

$$V(r,E) = V_R(r,E) + V_{SO}(r,E) + V_C(r,E) + \mathrm{i}\left[W_D(r,E) + W_S(r,E) + W_{SO}(r,E)\right], \quad (1)$$

where the different terms are

$$V_R(r,E) = -V_R(E) f(r, R_R, a_R), \quad (2)$$

$$V_{SO}(r,E) = \lambda_\pi^2 \left(\vec{L}\cdot\vec{S}\right) \frac{V_{SO}}{a_{SO}} \frac{1}{r} \frac{df(r, R_{SO}, a_{SO})}{dr}, \quad (3)$$

$$V_C(r) = \begin{cases} 0.7720448\,\frac{Z_d Z}{R_C}\left(3 - \frac{r^2}{R_C^2}\right) & \text{if } r < R_C, \\ 1.440975\,\frac{Z_d Z}{r} & \text{if } r \geq R_C, \end{cases} \quad (4)$$

$$W_D(r,E) = 4a_D W_D(E)\frac{df(r,R_D,a_D)}{dr}, \quad (5)$$

$$W_S(r,E) = -W_S(E) f(r,R_S,a_S), \quad (6)$$

$$W_{SO}(r,E) = \lambda_\pi^2 \left(\vec{L}\cdot\vec{S}\right)\frac{W_{SO}}{a_{SO}}\frac{1}{r}\frac{df(r,R_{SO},a_{SO})}{dr}, \quad (7)$$

$$f(r,R,a) = \left[1 + \exp\left(\frac{r-R}{a}\right)\right]^{-1}. \quad (8)$$

The different contributions to the phenomenological OMP are the central real part Eq. (2), the real part of the spin-orbit potential Eq. (3), the Coulomb potential Eq. (4), the volumen and surface contributions to the cental imaginary part, Eqs. (6) and (5), respectively, and the imaginary part of the spin-orbit potential Eq. (7). In both spin-orbit potentials, $\lambda_\pi^2 \simeq 2\,fm^2$ is the squared Compton wavelength of pion. The Woods-Saxon form factor is given by Eq. (8).

V_0	82.18	U_3	35.0
V_1	-0.148	W_{SO}	-0.206
V_2	-0.000886	a_R	0.809
V_3	-34.881	a_{SO}	0.813
V_4	1.058	a_d	0.465
V_{SO}	3.703	a_s	0.700
W_0	20.968	r_R	1.174
W_1	-0.0794	r_{SO}	1.234
W_2	-43.398	r_C	1.698
U_0	-4.916	r_D	1.328
U_1	0.0555	r_S	1.563
U_2	0.0000442		

TABLE I: Optical model potential parameters.

$V_R(E)$, V_{SO}, $W_D(E)$, $W_S(E)$ and W_{SO} are the potential depths and a_R, a_{SO}, a_D and a_S are the width of the potentials. The parametrization of Han *et al.* provides us with the following expressions.

$$V_R(E) = V_0 + V_1 E + V_2 E^2 + V_3\frac{N-Z}{A} + V_4 Z A^{-1/3} \quad (9)$$

$$W_D(E) = W_0 + W_1 E + W_2 E^2 + W_3\frac{N-Z}{A} \quad (10)$$

$$W_S(E) = \max\left[0, U_0 + U_1 E + U_2 E^2 + U_3\frac{N-Z}{A}\right] \quad (11)$$

$$a_D = a_d + 0.045A^{1/3} \quad (12)$$

$$a_S = a_s + 0.045A^{1/3} \quad (13)$$

Finally, the factors r_R, r_{SO}, r_C, r_D and r_S define the different radii entering in the OMP as

$$R_i = r_i A^{1/3} \qquad \text{for i = R, D, S, SO, C.} \quad (14)$$

Z, N and A are the proton, neutron and mass number of the nucleus, respectively, Z_d and E are the charge and the incident energy in the LAB system of the deuteron. The units of the potential depths and E are in MeV, while the lengths are in fm. The values of OMP parameters are given in Table I.

III. CALCULATIONS OF THE OBSERVABLES

In this section we will explain briefly the basis of the OM, which allow to estimate theoretically the measured quantities. Firstly, we have to calculate the scattering matrix elements. We start from time-independent Schrödinger equation,

$$\frac{\hbar^2}{2M}\nabla^2\Psi + (E - V(r))\Psi = 0, \quad (15)$$

where $V(R)$ is the OMP, E is the energy in the center of mass system and Ψ is the total wave function. If we assume spherical symmetry (r,θ,ϕ), Ψ can be written as an expansion of radial and angular partial wave functions,

$$\Psi = \sum_{l=0}^{\infty}\frac{u_l(r)}{r}Y_l^m(\theta,\phi). \quad (16)$$

We replace Ψ by the expansion of Eq. (16) into Eq. (15) and we obtain this two coupled equations,

$$\frac{d^2u_l^\pm(\rho)}{d\rho^2} + \left(K^\pm - \frac{l(l+1)}{\rho^2}\right)u_l^\pm(\rho) = 0, \quad (17)$$

where $u_l(\rho)^+$ and $u_l(\rho)^-$ are the complex radial wave function associated to m_S equal to +1/2 and -1/2, respectively. Remember that m_S is the spin quantum number and l is the angular momentum quantum number. The variable ρ is defined as $\rho = \frac{\sqrt{2\mu E}}{\hbar}r$ with μ the reduced mass of the deuteron-nucleus system. Last, $K^\pm$ are two conveniently defined complex functions, for $m_S = \pm 1/2$, which depend of the OMP $V(r)$. When r is greater than the matching radius, r_M, the nuclear terms of Eqs. (17) become irrelevant and only survives the long-range Coulomb part. In this scenario the asymptotic wave functions solution of Eqs. (17) are analytical and given by:

$$u_{l,as}^\pm(\rho) = [F_l(\rho) + iG_l(\rho)] + S_l^\pm[F_l(\rho) - iG_l(\rho)], \quad (18)$$

where F_l and G_l are the so-called regular and irregular Coulomb functions, respectively. The scattering matrix

elements $S^{\pm}$ are found by matching at ρ_M the numerical solutions of Eqs. (17), $u_l^{\pm}(\rho_M)$, which are called internal solutions, with the asymptotic solutions provided by Eqs. (18), $u_{l,as}^{\pm}(\rho_M)$. All solutions are calculated by means of a program that numerically integrates the two coupled Eqs. (17). The program used in this work is a modification of a program originally written in FORTRAN70 by P. E. Hodgson [10]. The original program was made to solve the nucleon-nucleus problem; therefore, we replaced the original OMP by a deuteron OMP.

Once the scattering matrix elements have been obtained, the spin-independent and spin-dependent scattering amplitudes are calculated as

$$A(\theta) = f_C(\theta) + \frac{1}{2ik}\sum_{l=0}^{\infty}[(l+1)S_l^+ + lS_l^- \text{-(2l+1)}]\ \exp(2i\sigma_l)P_l(\cos\theta) \quad (19)$$

and

$$B(\theta) = \frac{1}{2ik}\sum_{l=0}^{\infty}[S_l^+ - S_l^-]\exp(2i\sigma_l)P_l'(\cos\theta), \quad (20)$$

where $f_C(\theta)$ is the Coulomb scattering amplitude, $k = \frac{\sqrt{2\mu E}}{\hbar}$ is the wave number, σ_l is the Coulomb phase shift and $P_l(\cos\theta)$ are the Legendre polynomials. Finally, the differential cross section for elastic scattering (DCS) and the total reaction cross section (TCS) are given by

$$\frac{d\sigma}{d\Omega}(\theta) = \mid A(\theta) \mid^2 + \mid B(\theta) \mid^2 \quad (21)$$

and

$$\sigma_T = \frac{2\pi}{k^2}\sum_{l=0}^{\infty}[(l+1)(1-Re(S_l^+)) +\text{l(1-Re(S}_l^-\text{))}]. \quad (22)$$

In practice, partial waves with l greater than some maximum value, l_{max}, do not contribute significantly to the scattering amplitudes or cross sections, so the integration goes from 0 to l_{max}. In this work l_{max} has not exceeded 150 normally.

IV. RESULTS AND ANALYSIS

We first analyze the shape of real, imaginary and spin-orbit potentials as a function of the distance between the deuteron and the nucleus. In Fig.(1) we display the different components of the OMP in the case of a target of ^{64}Ni and deuterons of 100 MeV incident energy. In Fig. (1)(a) we observe that at the origin the nuclear term (V_R) provides the main contribution to the real potential and when the distance increases, it goes to 0. When it occurs, at approximately 9 fm, the Coulomb potential (V_C) becomes in the dominant term. It is well known that the nuclear force is a short-range interaction, while the Coulomb force is a long-range interaction, so the results are in accordance with the theory. In Fig. (1)(b) we observe a maximum of the volume absorption potential (W_S) at the origin that decreases at larger distances. In contrast, the surface absorption potential (W_D) does not contribute at the origin and reaches its maximum value at $r \sim 5-6$ fm. Both absorption potentials go to 0 for long distances. We observe that the combination of the surface and volume contributions lead to a full imaginary part of the OMP strongly peaked around 5-6 fm, which implies that the absorption is mainly produced at the nuclear surface.

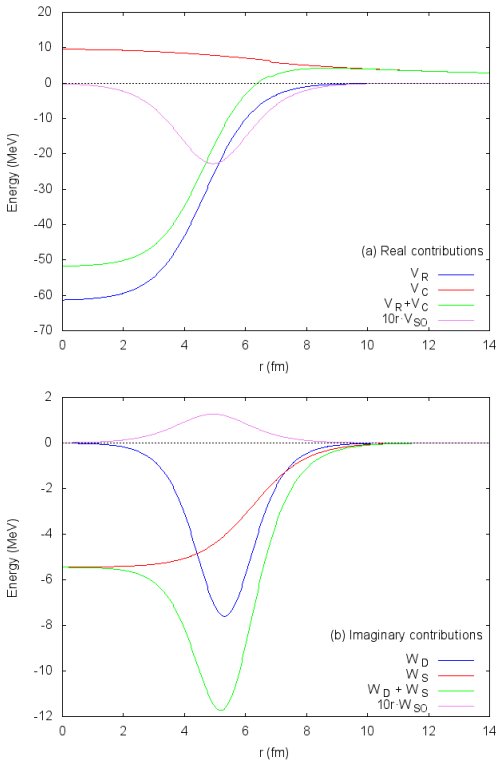

FIG. 1: Real (a) and imaginary (b) contributions to the OMP for a Ni-64 nucleus interacting with a 100 MeV incident energy deuteron. The real and imaginary contributions to spin-orbit potential are multiplied by a scale factor 10r to improve the visualization and to avoid divergences at the origin

The nuclear radius can be approximated by the well known formula $1.2A^{1/3}$, so the the Ni-64 nucleus surface is approximately located at $r \sim 5$ fm. Additionally, In Fig. (1) we observe that the real (V_{SO}) and imaginary (W_{SO}) contributions to the spin-orbit potential reach their maximum value at $r \sim 4-5$ fm (at the nuclear surface) and then go to 0. Finally, to summarize, in Fig. (1) we observe that the surface absorption and spin-orbit potentials are located in the surface, the volume absorption potential is located in the bulk and at long distances only Coulomb potential survives, which coincide with the theoretical expectations, so the results

obtained are satisfactory.

Table II shows the TCS predictions for different reactions and compares them with the experimental data. We have selected reactions that were not used in the adjustment process for this parametrization in order to assess its prediction ability.

Nucleus / E_d	$\sigma_T^{exp} \pm \delta\sigma_T^{exp}$	σ_T^{th}	$\Delta\sigma_T/\delta\sigma_T^{exp}$
Be-9 / 25.2	881±30	880.3	0.02
Be-9 / 37.9	811±35	807.8	0.09
Be-9 / 65.5	633±23	699.7	2.90
Be-9 / 97.40	536±26	607.2	2.74
Be-9 / 160	512±25	474.9	1.48
Al-27 / 13.35	1204±27	1267.0	2.33
Al-27 / 24.9	1230±55	1242.8	0.23
Al-27 / 160	996±50	880.2	2.32
Sc-45 / 13.6	1356±57	1401.8	0.80
Ti-48 / 13.6	1329±48	1417.6	1.85
V-51 / 13.6	1483±69	1432.0	0.74
Cr-52 / 13.6	1344±52	1430.2	1.66
Cr-53 / 13.6	1367±53	1437.8	1.34
Cr-54 / 13.6	1438±54	1445.1	0.13
Fe-54 / 12.3	1469±147	1374.7	0.64
Fe-56 / 12.3	1549±155	1391.2	1.02
Fe-58 / 12.3	1560±156	1406.7	0.98
Co-59 / 13.6	1609±41	1449.5	3.89
Co-59 / 25.2	1484±37	1603.5	3.23
Ni-60 / 13.6	1586±49	1444.0	2.90
Ni-64 / 12.46	1666±60	1430.9	3.92
Cu-63 / 13.31	1609±81	1430.9	2.20
Cu-65 / 13.6	1602±48	1465.9	2.84
Rh-103 / 25.2	1848±63	1911.7	1.01
Au-197 / 25.1	2028±65	2299.4	4.18
Bi-209 / 12.8	1185±183	910.2	1.50

TABLE II: Experimental data of TCS compared to results calculated by global potentials. The first column shows the target nucleus and the incident deuteron energy in MeV, the second and third columns show the experimental data with its uncertainty and the OMP results, respectively, in mb. The last column shows the ratio of TCS error of the prediction to uncertainty.

The error of the prediction is defined as the difference in absolute value between the theoretical results and the experimental data values, while the uncertainty its equal to the data standard deviation. To evaluate the goodness of a model we use the criterion that if the error of the theoretical estimate is less than twice the standard deviation, then the two values are consistent with each other. Otherwise, they are not. The predictions for nuclei lighter than Co-59 and low energies in general are correct while for high energies they are more erratic. The results are especially good for Be, Sc, Ti, V, Cr and Fe targets at low energies and are worse for Al nucleus. For nuclei of higher masses in general the results are less good except for Rh and Bi nuclei, which are less tan two standard deviations. Globally, the TCS computed using the Han *et al.* OMP describe reasonably well the experimental data.

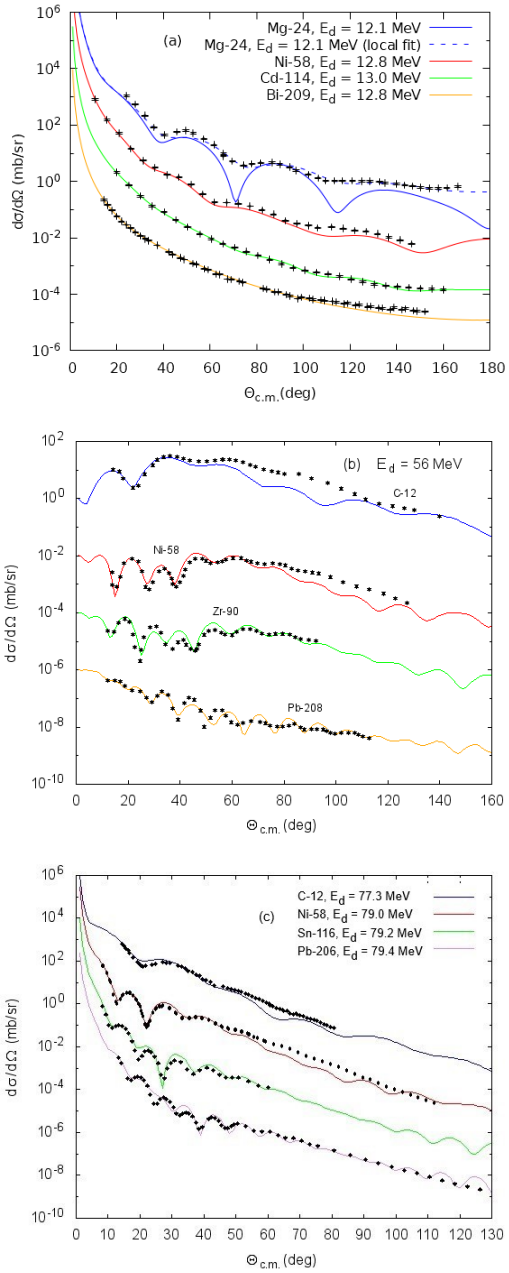

FIG. 2: DCS at 12-13 (a), 56 (b), 77-80 (c) MeV incident deuteron energies compared experimental data with calculated results by the global potentials. The results are offset by factors of 10.

Figs. (2) and (3) show the deuteron DCS for different target nuclei and incident deuteron energies. In Fig. (2)(a) we study the interaction between deuteron and Mg-24, Ni-58, Cd-114 and Bi-209 nuclei at incident en-

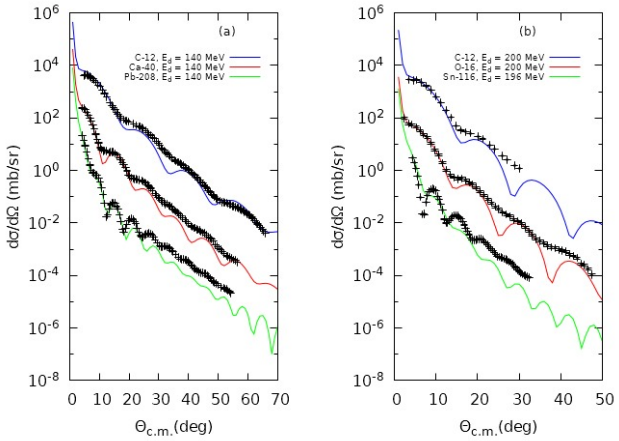

FIG. 3: DCS at 140 (a), 196-200 (b) MeV incident deuteron energies compared experimental data with calculated results by the global potentials. The results are offset by factors of 10.

ergies close to 13 MeV. The experimental DCS induced by deuterons of 12-13 MeV show a Rutherford pattern for all the considered nuclei, which is well reproduced by the global potential for heavier targets than Mg-24. For this nucleus (Mg-24) the DCS shows a diffractive pattern (solid line) pointing out that the Coulomb barrier is lower than the energy of the projectile. This can be cured with a *ad hoc* reduction of the real central potential by a factor 0.43 (local fit) for recovering the experimental trend (dashed line). In Fig. (2)(b) we study the interaction between deuteron and C-12, Ni-58, Zr-90 and Pb-208 nuclei at 56 MeV incident energy. The obtained results are in good agreement with the data for small angles and it are specially good for Ni-58 and Zr-90 from 20 to 80 angular degrees. The predictions for C-12 and Ni-58 at large angles underestimates the values of DCS. In Fig. (2)(c) we study the interaction between deuteron and C-12, Ni-58, Sn-116 and Pb-206 nuclei at incident energies close to 80 MeV. Theoretical results are consistent with experimental data. Results are especially well adjusted in the angle range from 10 to 50 angular degrees, where the DCS oscillations are predicted by the OMP. In Fig. (3)(a) we study the interaction between deuteron and C-12, Ca-40 and Pb-208 nuclei at 140 MeV incident energy. For forward angles the theoretical results are in reasonable agreement with experimental data while for larger angles the DCS values are underestimated. In Fig. (3)(b) we study the interaction between deuteron and C-12, O-16 and Sn-116 nuclei at 200 MeV incident energy. The OMP predictions are reasonable correct for angles up to 10 angular degrees, however results are erratic for larger angles. At these high energies the theoretical DCS are, in general, smaller tan the experimental data for angles larger than 15-20 degrees. This implies that the absorption predicted by the model is too strong.

V. CONCLUSIONS

We have reached three main conclusions after completing this project. First, the OM is a very useful theoretical tool that allows us to obtain reasonably accurate information about nuclear reactions through relatively simple calculations. Second, model proposed by Han *et al.* applied to deuteron induced reactions different from the ones used in the fit of the model, predict, on the one hand, reasonable TCS for different target nuclei and incident energies, especially for intermediate nuclei and low energies. On the other hand, this model reproduces DCS quite well in a wide range of target nuclei and incident energies, especially for nuclei heavier than Mg-24 and energies up to 100 MeV. Finally, the third conclusion, in the elastic scattering of deuterons with incident energy of 12 MeV we have observed that the global parametrization may present failures in some reactions, which can be solved by introducing *ad hoc* modifications in the potential (local fit).

VI. ACKNOWLEDGEMENTS

I would like to express my special gratitude to my advisor, Dr. Xavier Viñas, for supporting me in this study. He provided me with all the information I needed and resolved any questions I might have about realizing the project. Secondly, I would also like to thank my parents and friends who helped me in finalizing this project within the limited time frame.

[1] P.E. Hodgson, *The Optical Model of Elastic Scattering* (Clarendon, Oxford, 1963).
[2] R.L. Varner and W.J. Thompson, T.L. McAbee, E.J. Ludwig and T.B. Clegg, Phys. Rep. **201**, 57 (1991).
[3] F.D. Becchetti Jr. and G.W. Greenlees, Phys. Rev. **182**, 1190 (1969).
[4] A.J. Koning, J.P. Delaroche, Nucl. Phys. **A713**, 231 (2003).
[5] Alliot C *et al.*, Frontiers in Medicine (Lausanne) **2**, 31 (2015).
[6] W. W. Daehnick, J. D. Childs, and Z. Vrcelj, Phys. Rev. C **21**, 2253 (1980).
[7] J. Bojowald, H. Machner, H. Nann, W. Oelert, M. Rogge, and P. Turek, Phys. Rev. C **38**, 1153 (1988).
[8] Yinlu Han, Yuyang Shi, and Qingbiao Shen, Phys. Rev. C **74**, 044615 (2006).
[9] Experimental Nuclear Reaction Data (EXFOR), https://www-nds.iaea.org/exfor/.
[10] P.E. Hodgson and E. Sartori, NEANDC-198-U, INDC(NEA)5.